Received: 24 March 2021 | Accepted: 7 July 2021

DOI: 10.1002/ajb2.1745

RESEARCH ARTICLE

American Journal of Botany

Functional responses to climate change may increase invasive potential of *Carpobrotus edulis*

Josefina G. Campoy[1] | Margarita Lema[1] | Erola Fenollosa[2,3] | Sergi Munné-Bosch[2,3] | Rubén Retuerto[1]

[1]Departamento de Bioloxía Funcional, Facultade de Bioloxía, Universidade de Santiago de Compostela, Santiago de Compostela, A Coruña 15782, Spain

[2]Department of Evolutionary Biology, Ecology and Environmental Sciences, Faculty of Biology, University of Barcelona, Barcelona, Spain

[3]Biodiversity Research Institute (IrBio), Faculty of Biology, University of Barcelona, Barcelona, Spain

Correspondence

Josefina G. Campoy, Departamento de Bioloxía Funcional (Área de Ecoloxía), Facultade de Bioloxía, Universidade de Santiago de Compostela, Santiago de Compostela, A Coruña 15782, Spain.
Email: josefina.gonzalez@usc.es and josefina.gonzalez.campoy@gmail.com

Abstract

Premise: Biological invasions and climate change are major threats to biodiversity. It is therefore important to anticipate how the climate changes projected for Southern Europe would affect the ecophysiological performance of the invasive South African plant, *Carpobrotus edulis* (ice plant or sour fig), and its capacity to undergo rapid adaptive evolution.

Methods: We manipulated the climate conditions in a field plot located on the island of Sálvora (northwest of the Iberian Peninsula) to establish a full factorial experiment with *C. edulis* plants transplanted from four native (southern African) and four invasive (northwestern Iberian Peninsula) populations. Throughout 14 months we measured growth and functional traits of this species under two temperatures (control vs. increased), and two rainfall levels (control vs. reduced).

Results: Temperature increased photochemical efficiency and relative growth rate of *C. edulis*. Rainfall modulated some of the effects of temperature on C and N isotopic composition, and pigment contents. Invasive populations showed lower root mass allocation and higher survival rates, as well as increased water use efficiency, lipid peroxidation, chlorophyll, and xanthophyll cycle pigment contents than native populations.

Conclusions: The increased growth and physiological performances observed under our experimental conditions suggest that the expected climate changes would further promote the invasion of *C. edulis*. Differences between native and invasive genotypes in survival and functional traits revealed that populations have diverged during the process of invasion, what gives support to the invasiveness hypothesis. Our findings highlight the importance of analyzing intraspecific variability in functional responses to better predict how invasive species will respond to environmental changes.

KEYWORDS

Aizoaceae, biomass allocation patterns, ecophysiology, evolutionary change, global warming, ice plant, invasive species, isotope composition, photoprotection, pigment contents

Biological invasions and climate change are among the greatest drivers of global change (Schröter et al., 2005). Plant invasions can significantly alter the composition and structure of native communities and the functioning of ecosystems, threatening biodiversity and ecosystem services (Vitousek et al., 1997; Mack et al., 2000; Sala et al., 2000). Climate change may further enhance invasion processes by affecting initial introduction, establishment, and spread (Walther et al., 2009; Díez et al., 2012). The concurrent effects of these major agents of global change are expected to impose additional pressure on the stability of ecosystems (Sala et al., 2000; EEA, 2017).

The climate, operating through basic physiological processes, is the primary force governing plant distribution (Walter, 1975; Woodward, 1987; Retuerto and Carballeira, 2004). The average temperature in Europe is projected to increase by 1.0–5.5°C during the course of the

21st century (2071–2100 compared to the 1971–2000 mean). Climate models for the same period project a decrease of up to about 40% in rainfall in Southern Europe (IPCC, 2014: EEA, 2017). The predicted changes are therefore expected to affect the physiology of invasive species and to alter their competitive interactions, and thus their ability to persist in a given location (e.g., Bradley et al., 2010; Matesanz and Valladares, 2014). In fact, there is increasing evidence that predicted changes in climate, especially rising global temperatures and a higher frequency of extreme meteorological events such as droughts, are likely to alter the distribution and prevalence of some invasive plant species (e.g., Thuiller et al., 2007; Walther et al., 2009; Bellard et al., 2013; EEA, 2017). However, invasive plant studies involving experimental manipulation of climatic conditions are scarce.

The relatively high prevalence of competitively advantageous functional traits (Matzek, 2012) and high phenotypic plasticity of invasive plants (Richards et al., 2006; Hulme, 2008; Castillo et al., 2018), may allow invaders to take advantage of the warmer and drier conditions of the new climatic scenarios (Dukes and Mooney, 1999; Díez et al., 2012; Matzek, 2012). If so, climate change could increase their growth and consequently facilitate the expansion and the potential effect of invasive species on ecosystems. In the context of rapid climate change endangering biodiversity, it is essential to anticipate how the new climate scenarios would affect the performance of invasive plants. This information would be useful for predicting the potential distribution of invaders and for designing appropriate management strategies.

In addition to identifying those traits that make a plant invasive under climate change, it is urgent to know the evolutionary processes that allow them to become invasive (Brodersen et al., 2008). To develop a truly mechanistic understanding of how introduced species spread worldwide, Thompson (1998) proposed considering rapid evolution as an ecological process. Other studies have considered that the evolution of invasiveness after colonization may be more important to explain successful invasions than an innate ability to colonize new landscapes (Ellstrand and Schierenbeck, 2000; Lee, 2002).

Several studies have documented rapid evolutionary changes in invasive species on a scale of years or even decades after introduction in new territories (Sax et al., 2007; Nguyen et al., 2016). These evolved changes may speed up adaptive processes by improving the performance of invasive species in the introduced range or under the emerging environmental conditions, leading to divergence of important adaptive traits between invasive and native populations of a species (e.g., Caño et al., 2008; Matesanz et al., 2010). However, despite the importance of physiological filters in the adaptive success of invasive species to new areas, very few studies have investigated differences in physiological traits between invasive and native populations of a single species (Maron et al., 2007; Brodersen et al., 2008; Roiloa et al., 2016).

Our model species, *Carpobrotus edulis* (L.) N.E. Br. (Aizoaceae), is a good example of an invasive perennial plant that is threatening the diversity of coastal ecosystems. This South African plant was first introduced to Europe more than one hundred years ago, and since then, many studies have focused on the effects it has on the invaded ecosystems (reviewed by Campoy et al., 2018). In addition, according to Thuiller et al. (2005), the area that is potentially suitable for *C. edulis* appears to be wider than at present and it could be increased greatly in the future. To our knowledge, this is the first mechanistic study to use manipulated field conditions to evaluate how the widespread invasive plant *C. edulis*, now present on Africa, Asia, America, Europe, and Oceania (Campoy et al., 2018), will respond to climate change projections for Southern Europe (IPCC, 2014; EEA, 2017). Specifically, we addressed two main questions: (1) Will the predicted increased temperature and decreased rainfall in Southern Europe enhance growth and physiological performance of *C. edulis*? Given the flexible photosynthetic physiology of this facultative C_3-Crassulacean acid metabolism (CAM) species (e.g., Winter and Holtum, 2014), and its presumably high tolerance to drought and elevated temperatures (Campoy et al., 2018), we expect it takes advantage of the warmer and drier conditions, increasing its growth, water use, and photochemical efficiencies under the new climatic scenarios. (2) Have invasive populations of *C. edulis* in the Iberian Peninsula diverged during the invasion process from those populations remaining in the warmer and drier native habitats in South Africa? Based on previous studies on this species (Roiloa et al., 2016) and other invasive species (Sax et al., 2007; Nguyen et al., 2016), which suggest rapid adaptive changes during invasion processes, we expect strong genotype by environment interactions in survival and functional traits. South African genotypes, growing in warmer and drier conditions than invasive genotypes, would therefore outperform the Iberian genotypes under the predicted climatic scenarios, but underperforming them under control conditions. Such genetic differences could have emerged by local adaptation as a result of adaptive evolution, genetic drift, genetic bottlenecks, and admixtures, among others.

MATERIALS AND METHODS

Study species

Carpobrotus edulis (L.) N.E. Br. (Aizoaceae) is a succulent perennial plant with a mat-forming habit native to southern Africa (Wisura and Glen, 1993) (Appendix S1). This diploid species ($2n = 2x = 18$) (Gonçalves, 1990) was introduced across the five worldwide Mediterranean climate regions for ornamental and soil stabilization purposes, and since then it has become invasive in many coastal habitats (review in Campoy et al., 2018). The success of *C. edulis* as an invader has been explained by its reproductive strategies, including

hybridization (e.g., Vilà and D'Antonio, 1998; Suehs et al., 2004), intense clonal reproduction (Campoy et al., 2018), large seed bank (Chenot et al., 2014), and high rates of seed dispersal (D'Antonio, 1990; Bourgeois et al., 2005). The significant morphological and ecophysiological plasticity of *C. edulis* (Campoy et al., 2017; Fenollosa et al., 2017, 2019; Fenollosa and Munné-Bosch, 2019) is also an important feature explaining its tolerance to a wide range of ecological constrains.

Sampled populations and experimental design

The study was conducted on the island of Sálvora (42°28′44″N, 9°0′34″W), within the National Park of the Atlantic Islands of Galicia (northwest of the Iberian Peninsula) (Appendix S2). The island's climate has been described as "Mediterranean sub-humid of Atlantic tendency" (Allué, 1966) and "Warm temperate, with dry and warm summers" (*Csb)*, under the Köppen–Geiger climate classification (Kottek et al., 2006). The mean annual rainfall is 1193 L/m^2 and the mean temperature of the warmest (August) and the coldest (December) month vary from 20°C to 10°C, respectively (www.meteogalicia.es). The Western Cape's climate in South Africa is also under the Köppen–Geiger climate classification *Csb* (Kottek et al., 2006). The mean annual rainfall is 576 L/m^2 (Mostert et al., 2017) and the mean temperature of the warmest (February) and the coldest (July) month vary from 22°C to 12°C, respectively (Campoy et al. 2018, and references therein).

In the study area, we delimited a plot (21 m long × 12 m wide) over a secondary dune (IGME, 2014) by a fence, to exclude large herbivores. The center of the plot was approximately 75 m from the foreshore. Thirty-two subplots (1.55 m × 1.75 m) regularly spaced were demarcated inside this plot (Appendix S3) to establish a full factorial experimental design with three factors: region of ramet collection (native vs. invaded region), temperature (control vs. increased temperature), and rainfall (control vs. reduced rainfall). Eight subplots were sequentially assigned to each the following climatic conditions: increased temperature (IT), reduced rainfall (RR), increased temperature with reduced rainfall (IT + RR), and control (C) (Appendix S4). We installed open top chambers (OTCs), which are typically used in warming experiments (e.g., Hollister and Webber, 2000; Maestre et al., 2013), in eight of the subplots (IT). The OTCs, made of methacrylate, were hexagonal with sloping sides of 40 cm × 50 cm × 70 cm, and covered an area of 1.27 m^2. The bottom edge of all chambers was elevated ~5 cm above the soil surface for ventilation and to prevent excessive temperatures being reached (Appendix S4a). These chambers were designed to increase the ambient temperature by approximately 2.0°C, a realistic scenario for the study area, according to the predictions of the regional atmospheric "Pronóstico a Mesoescala" (PROMES) model (Castro et al., 1993). To achieve the rainfall reduction predicted in the study area, we placed methacrylate rainfall collectors (Appendix S4b), based on the design of Yahdjian and Sala (2002), in eight of the subplots (RR). The vertical projection of the collectors covered an area representing approximately 33% of the surface of the subplot and reducing the amount of rain reaching the soil surface by the same percentage. The water intercepted by the collectors was channeled through a flexible pipe into storage tanks for periodic quantification (Appendix S4e, f). To examine the combined effects of increased temperature and reduced rainfall, we installed an OTC below the rainfall collectors in another eight subplots (IT + RR) (Appendix S4c). Finally, the eight remaining subplots represented the current climatic conditions (C). To ensure that plants grew in the same area in all treatments, we delimited a hexagonal area of 1.27 m^2 in the center of the subplots assigned to the control climate and reduced rainfall treatments (Appendix S4d).

The experimental plant material was sampled between January and April 2015 from eight populations (Appendix S5), four from the native area (Cape Region, South Africa) and four from the invaded area (northwest of the Iberian Peninsula, Southern Europe). To have a more comprehensive illustration of the genetic variability we selected, within each population, 36 clumps separated at least 25 m from the others. *Carpobrotus edulis* forms compact clumps, and it is reasonable to assume that each separated clump represents a different genotype. Thus, we collected the most apical part of a stolon with four ramets (i.e., units or modules [sensu Harper, 1977]) for a total of 288 potential genotypes. From these, 128 (64 per region and 16 per population) were haphazardly selected for the study. The sampled plants were transplanted into trays filled with dune sand and maintained in a glasshouse at the University of Santiago de Compostela. These plants were grown under natural light conditions until the start of the experiment. To prevent hydric stress, plants were watered according to their requirements (approximately once or twice per week).

In September 2015, after the natural vegetation growing in the 32 subplots was carefully removed, we transplanted one *C. edulis* genet in each of the four quadrants of each subplot. Each genet was composed by the three most apical ramets (15 cm long) by excising them from the plant stock ($n = 128$ genets) to guarantee that each plant was at the same stage of development. Specifically, we haphazardly assigned four genets to each subplot: two from populations from the invaded area and two from populations from the native area. Thus, 16 genets per region (four per population) were grown under each of the four climatic treatment (eight subplots per treatment).

Because of mortality and damage by predation (Appendix S6a, b), the number of individuals considered in the statistical analysis (except for survivorship) was reduced to the 48 genets (24 from the native and 24 from the invaded regions) that remained completely healthy at the end of the experiment, i.e., six replicates for each treatment combination. These replicates came from the four populations in their respective region, so all populations were represented in our final design.

To monitor temperature and relative humidity in the experimental subplots, 12 sensors were placed 5 cm above the soil surface, three for each treatment (iButton Hygrochron DS1923, Maxim Integrated Products, Inc., San José, California, USA). Soil temperature and humidity were monitored at 5–10 cm depth in the center of four subplots, one per treatment, using sensors (S-SMD-M005 Soil Moisture and S-TMB-M006 Temperature Smart Sensors; Onset, Bourne, Massachusetts, USA) connected to continuous data loggers (HOBO H21-002-HR Data Logger; Onset, Bourne, Massachusetts, USA) (Appendix S6c, d).

Survivorship

Throughout the experiment, we recorded the survivorship of *C. edulis* plants from both native and invaded regions in each treatment as the cumulative proportion of surviving plants between the start (September 2015) and the end of the experiment (November 2016).

Growth and biomass allocation

Before the start of the experiment, we determined the fresh weight (FW) of unrooted plants to the nearest 0.0001 g (Mettler AJ100, Mettler-Toledo, Greifensee, Switzerland). At the end of the experiment, we determined the FW and the dry weight (DW) of each plant (after drying at 60°C to constant weight). Each dried plant was separated into shoots (including leaves and stolons) and roots to determine the proportion of biomass allocated to roots (root-to-shoot ratio [RSR]), calculated as RSR = root dry mass/shoot dry mass. To correct for the larger initial size of plants from the invaded region ($F_{1,47} = 11.99$; $P = 0.001$), plant growth (aboveground mass + root mass) was determined as the relative growth rate (RGR). The RGR, defined as the biomass gain per unit of biomass and time (Villar et al., 2004), was calculated as [ln (dry weight t_2) – ln (dry weight t_1)]/($t_2 - t_1$), where t_1 is the initial time and t_2 is the final time. The initial dry weight was estimated from the ratio between DW and FW of 10 additional plants per population and region ($n = 80$).

Physiological traits

Leaf carbon and nitrogen content and isotopic composition

A composite sample of leaves from the three apical-most ramets in each plant was cleaned of organic debris and dried to constant weight (at 40°C for six days). The samples were then ground in a ball mill (Mixer Mill 400, Retsch GMBH, Haan, Germany), to produce a homogeneous fine powder. The C and N percentages of dry mass and the molar $^{15}N/^{14}N$ ($\delta^{15}N$) and $^{13}C/^{12}C$ ($\delta^{13}C$) ratios were determined in these samples (~2–3 mg dry wt) in an elemental analyzer (Flash EA 1112 Series, Thermo Fisher Scientific Inc., Waltham, Massachusetts, USA) coupled to an isotope ratio mass spectrometer (MAT253, ThermoFinnigan, Bremen, Germany) by the Research Support Services of the University of A Coruña (Spain). Carbon and N isotope ratios were expressed relative to the composition of a standard (Pee Dee belemnite [PDB] $CaCO_3$ for C, and atmospheric N for N). The δ values (‰) were calculated as $[(R_{sam}/R_{std}) - 1] \times 1000$, where R refers to the $^{13}C/^{12}C$ or $^{15}N/^{14}N$ ratio in the plant sample and standard, respectively. Polyethylene (International Atomic Energy Agency [IAEA C6]) and $(NH_4)_2SO_4$ (IAEA N1) were used as secondary international isotope standards for C and N, respectively. The $\delta^{13}C$ values were transformed into $\Delta^{13}C$ values by using the following expression: $\Delta^{13}C = (\delta^{13}C_{air} - \delta^{13}C_{plant})/(1 + \delta^{13}C_{plant})$, assuming a $\delta^{13}C$ air value of −8‰ on the PDB scale (Farquhar et al., 1989). By determining the ^{13}C isotope discrimination ($\Delta^{13}C$), we can obtain a time-integrated measurement of water use efficiency (WUE), i.e., the ratio assimilation rate: transpiration rate (Farquhar et al., 1989).

Chlorophyll fluorescence and leaf reflectance

We measured chlorophyll fluorescence yield and leaf reflectance in all plants at intervals of approximately two months, between November 2015 and November 2016.

Chlorophyll fluorescence was measured on a fully developed, healthy leaf of each plant, with a portable pulse amplitude modulated fluorometer (Mini-PAM; Heinz Walz, GmbH, Effeltrich, Germany). We determined "the maximum quantum yield of Photosystem II" (PSII) assessed by $F_v/F_m = (F_m - F_0)/F_m$, where F_m and F_0 are defined as the maximum and minimal fluorescence yield, respectively, of a dark-adapted sample (Bolhàr-Nordenkampf et al., 1989). Leaves were dark-adapted for one hour before the F_v/F_m was recorded (on dark leaf clips) (Heinz Walz, GmbH), to ensure that all PSII reaction centers were open. The maximum quantum yield estimates the efficiency of excitation energy capture by open PSII reaction centers and is correlated with the amount of carbon gained per unit of light absorbed (Bolhàr-Nordenkampf and Öquist, 1993). A decrease in F_v/F_m values, with control values typically in the range 0.75–0.85, has been considered symptomatic of photoinhibitory damage (Bolhàr-Nordenkampf et al., 1989).

Concurrent with the fluorescence measurements, the reflectance spectra were recorded within a wavelength range of 300–1000 nm, with a portable spectrometer (Unispec, PP Systems, Haverhill, Massachusetts, USA). Leaf reflectance was calculated by dividing the spectral radiance of the leaf by the radiance of a reflective white standard (Spectralon Reflectance Standard, Labsphere, North Sutton, New Hampshire, USA). Reflectance data were processed using AVICOL v.6 software (Gomez, 2006) to compute some indices that are closely related to functional processes. The "red edge index" (λ RE) represents the wavelength of maximum slope in the increase of reflectance

from red to near infrared (between 680 and 750 nm) (Lichtenthaler et al., 1996). The position of the red edge is considered the best indicator of chlorophyll content at leaf level (Filella and Peñuelas, 1994). The "structural independent pigment index" (SIPI) was computed as $(R_{800} - R_{445})/(R_{800} - R_{680})$ (Peñuelas and Filella, 1998), where R represents reflectance at a given wavelength. This index provides a very good semi-empirical estimation of the carotenoid-to-chlorophyll *a* ratio for several species (Peñuelas et al., 1995a). The "yellowness index" (YI), calculated as $YI = -10\ (R_{580} - 2R_{624} + R_{668})/44^2$, was formulated to indicate chlorosis in stressed leaves by measuring changes in the shape of reflectance spectra at approximately 600 nm (Adams et al., 1999). A scaling factor of −10 was included to indicate increasing yellowness within increasingly positive values (Adams et al., 1999). The "photochemical reflectance index" (PRI_{531}) was determined as $(R_{531} - R_{570})/(R_{570} + R_{531})$ (Gamon et al., 1992; Peñuelas et al., 1995b), where R represents reflectance at a given wavelength. Previous studies have demonstrated that PRI is inversely correlated with the dissipation of excess radiation energy as heat (Guo and Trotter, 2004). Finally, the "water index" (WI_{900}) was calculated as the R_{900}/R_{970} ratio (Peñuelas et al., 1997), where R_{970} reflects variations in leaf water content, and R_{900} is used as a reference.

Biochemical analysis: pigment contents, photoprotection, and stress-related phytohormones

In November 2016, one healthy and fully developed leaf was removed from each plant ($n = 48$). The leaf material was frozen in situ in liquid nitrogen, temporarily stored at −80°C, and later sent on dry ice to the University of Barcelona for analysis.

For a description of the photoprotective capacity and the redox status of the chloroplast, we determined the content of photosynthetic pigments and tocopherols (antioxidant molecules), the extent of lipid peroxidation, and stress-related phytohormones. The levels of photosynthetic pigments (including chlorophylls *a* and *b* [Chl*a* and Chl*b*, respectively], the ratio of chlorophylls *a* to *b* [Chl *a*/*b*], total chlorophyll [Chl_T], xanthophylls, β-carotene, and the ratio of carotenoids [Car] to Chl_T) and tocopherols (α-TOC and γ-TOC) were measured by high performance liquid chromatography (HPLC), as described by Munné-Bosch and Alegre (2000) and Amaral et al. (2005), respectively. The total xanthophyll pool (VAZ) was estimated as the total violaxanthin (Vx), antheraxanthin (Ax), and zeaxanthin (Zx) contents. The de-epoxidated state of the xanthophyll cycle (DPS) was calculated as Zx + 0.5Ax/VAZ.

The same methanolic extract with 0.01% butylated hydroxytoluene was used to estimate lipid peroxidation (associated with oxidative stress) by measuring the accumulation of lipid hydroperoxides in a modified ferrous oxidation-xylenol orange assay, as described by DeLong et al. (2002). The contents of different stress-related phytohormones, including abscisic acid (ABA), salicylic acid (SA) and jasmonic acid (JA) were also measured in the same plant extract, by ultra-HPLC coupled to electrospray ionization tandem mass spectrometry (UHPLC/ESI-MS/MS) as described by Müller and Munné-Bosch (2011). Deuterium-labeled compounds for all phytohormones were used as internal standards to estimate recovery rates for each sample.

Statistical analyses

Linear mixed models (LMM) were constructed for each variable, with region of ramet collection (hereafter "region"), temperature and rainfall as fixed effects, and populations as a random effect nested within region. Because of the repeated measure nature of leaf reflectance (ʎ RE, SIPI, YI, WI_{900}, and PRI_{531}) and chlorophyll fluorescence (F_v/F_m), time was considered as a random effect. The differences between treatments were determined by including random intercepts in the models. Because fluorescence and reflectance measurements are usually affected by solar irradiation and temperature conditions of the measuring days, mean values of these climatic variables (the latest four days; data taken from www.meteogalicia.es) were included as covariates to consider any potential effect on dependent variables. Random effects and covariate importance were both tested by comparing the more complex model with the simpler model and applying a χ^2 test of the explained deviance gained by the complex model. The simpler models were selected when no significant differences were detected between these and the more complex models. The LMM parameters were estimated using a restricted maximum likelihood (REML) approach.

Pairwise comparisons were made using a Monte Carlo–corrected *P* value based on a multivariate normal *t*-test distribution (mvt method). Analysis of variance (ANOVA) tables (type III) for LMM, estimated using Satterthwaite degrees of freedom, were used to examine the effects of treatments on variables. Prior to analyses, we checked for normality and homoscedasticity of the data by using Kolmogorov–Smirnov and Levene tests, respectively. Variables that did not meet the model assumptions, were normalized by applying Box–Cox transformations, except for the SIPI, YI, and PRI_{531} indices, which were normalized by Yeo-Johnson transformations (Box and Cox, 1964). Goodness of fit was tested using QQ-plots, histograms, and residuals vs. fitted plots over the studentized residuals.

To establish the independence between climatic treatments or regional groups (native vs. invaded) and plant survival, we performed a nonparametric analysis (Fisher's test) considering the initial 128 genets. Subsequently, regional survival functions were estimated using the nonparametric Kaplan-Meier estimator. A nonparametric test was used to compare the survival distributions of two regional curves (log-rank test). Finally, a semiparametric Cox proportional hazards model was adjusted to estimate adjusted odd ratio. The proportional risks assumption was checked using Schoenfeld residuals. All statistical analyses were performed in R (R Core Team, 2015). Models

were calculated with the LME4 package (Bates et al., 2014). Estimated marginal means were calculated using the emmeans package (Lenth, 2019) and analyses for plant survival were performed using base and survival R packages (Therneau and Grambsch, 2000; R Core Team, 2015; Therneau, 2021). In all analyses, a P value ≤ 0.05 was considered as statistically significant.

RESULTS

Climatic treatment effects on environmental variables

Throughout the study period, the OTCs increased the air temperature by 2.0°C on average (Appendix S7a) and the soil temperature (5–10 cm depth) by 1°C (Appendix S8a) on average. Temperature effects were maximized from May to September, when air temperature was increased by up to 9°C (Appendix S7a, c) and soil temperature by up to 3.3°C on some days (Appendix S8a, c). The reduced rainfall treatment did not substantially alter the air or soil temperature, because the average differences between the reduced rainfall and control treatments throughout the study period were below 0.3°C in both cases (Appendix S7a, S8a). The rainfall collectors decreased the air humidity by 4.8% (Appendix S7b, d) on average, and soil humidity by 1.17% (Appendix S8b, d) on average. The reduction in air and soil humidity by collectors was most notable during rainfall events registered from June to September on the island of Sálvora (Appendix S9), when air humidity was decreased by up to 30% (Appendix S7b, d) and soil humidity by up to 13% (Appendix S8b, d).

Survivorship

Plant survival was not associated with climatic treatments ($P = 0.230$), but with the region (Fisher's test, $P \leq 0.001$). Differences in survival between native and invasive populations were significant (log-rank test, $P \leq 0.001$). The region was also significant (Cox regression model, $P \leq 0.001$), with a hazard ratio of 0.1290, indicating a strong association between the region and an increased risk of death. Plants from the invaded region were seven times more likely to survive than plants from the native region (95% confidence interval: 2.3–26.1; Appendix S10). Schoenfeld residues of the model showed no trend against transformed time, therefore it is assumed that the risks are proportional ($P > 0.05$).

Growth and biomass allocation

Irrespective of region, temperature significantly increased the RGR by 19% ($F_{1,44} = 4.74$; $P = 0.035$; $R^2 = 0.11$; Figure 1A), total dry mass by 70% ($F_{1,44} = 5.06$; $P = 0.030$; $R^2 = 0.16$) and shoot dry mass by 71% ($F_{1,44} = 5.23$; $P = 0.027$; $R^2 = 0.17$). We did not detect significant effects of rainfall for the biomass variables (P values were always >0.456; see Appendix S11 for boxplots showing the distribution of data). *Carpobrotus edulis* plants from the native and the invaded region did not differ in RGR, but they did differ in RSR, which was 37% lower in plants from the invaded region ($F_{1,44} = 13.21$; $P = 0.001$; $R^2 = 0.24$; Figure 1B).

Physiological traits

Leaf carbon, nitrogen content, and isotopic composition

The $\Delta^{13}C$ values were significantly lower in plants from the invaded region than in plants from the native region ($F_{1,43} = 5.19$; $P = 0.028$; Figure 2A). We did not detect significant effects for the percentage of N or the C/N ratio

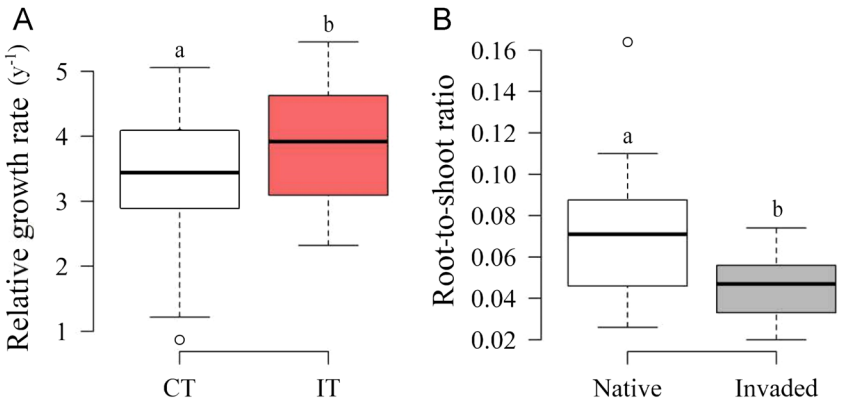

FIGURE 1 (A) Temperature effects (control [CT] vs. increased [IT]) on the relative growth rate (RGR [year^{-1}]) of *C. edulis*, and (B) region effects (native vs. invaded) on the root-to-shoot ratio (RSR = root dry mass/shoot dry mass) of *C. edulis*. The boxplots show the median, interquartile range, minimum, maximum, and the suspected outliers; $n = 24$. Different lowercase letters indicate significant differences at $P < 0.05$ (see text for statistics)

(P values were always >0.097; see Appendix S12). Temperature significantly reduced the percentage of C of plants ($F_{1,44} = 6.01$; $P = 0.018$; $R^2 = 0.21$; Figure 2B).

Irrespective of region, the effect of temperature on $\Delta^{13}C$ and $\delta^{15}N$ values depended on rainfall (Figure 2C, D, and Appendix S12 for boxplots showing the distribution of data). Temperature significantly increased $\Delta^{13}C$ values and decreased the $\delta^{15}N$ values of plants under control rainfall, but surprisingly did not affect either $\Delta^{13}C$ or $\delta^{15}N$ values of plants under reduced rainfall ($\Delta^{13}C$: $F_{1,44} = 4.46$; $P = 0.041$; $R^2 = 0.33$ and $\delta^{15}N$: $F_{1,43} = 7.51$; $P = 0.009$; $R^2 = 0.21$).

Leaf spectral reflectance and chlorophyll fluorescence

Temperature significantly increased the photochemical efficiency of plants (PRI_{531}: $F_{1,369} = 7.63$; $P = 0.006$; $R^2 = 0.53$; Figure 3A) and decreased the proportion of carotenoids to chlorophyll *a* (SIPI: $F_{1,368} = 11.66$; $P = 0.001$; $R^2 = 0.68$; Figure 3C). The YI showed a significant lower level of chlorosis in plants grown at increased temperature than in those grown at control temperature ($F_{1,373} = 10.41$; $P = 0.001$; $R^2 = 0.61$; Figure 3B). The carotenoid-to-chlorophyll *a* ratio was significantly lower in plants grown under reduced rainfall than in those grown under control rainfall (SIPI: $F_{1,369} = 9.65$; $P = 0.002$; Figure 3D).

We did not detect any significant effect of region or climatic treatments on F_v/F_m and WI_{900} (P always >0.113).

Irrespective of region, the reflectance and fluorescence indices showed that the photoprotective strategies of *C. edulis* varied over time. The YI and SIPI values revealed a significant increase in photoprotective pigments during spring and summer. By contrast, values for F_v/F_m showed a similar trend to that observed for PRI_{531} and ʎ RE indices, with lower values during spring and summer than in autumn and winter (Appendix S13). In July, plants suffered photoinhibition when grown in IT conditions, as indicated by their F_v/F_m values falling below 0.75 (Appendix S13e). Regarding plant water content, *C. edulis* maintained the highest levels of leaf water content, estimated by the WI_{900} reflectance, during spring and summer, and the values decreased in autumn and winter, especially in March (Appendix S14c).

Irrespective of time, the ʎ RE values showed that chlorophyll contents were significantly higher in plants from the invaded region than in plants from the native region ($F_{1,369} = 8.89$; $P = 0.003$), but the magnitude of this effect depended on the interaction of temperature by rainfall ($F_{1,369} = 5.59$; $P = 0.019$; $R^2 = 0.51$; Figure 4).

Irrespective of temperature and rainfall, PRI values were lower and YI values were higher in plants from the native region than in plants from the invaded region during May and June (Appendix S14a, c).

Biochemical analysis

Pigment contents

At the end of the experiment, the biochemical analysis did not reveal any significant effects of region, temperature, or rainfall for Chl*a*, Chl*b*, Chl *a*/*b*, Chl_T, and Car/Chl_T (P always >0.054) nor for lutein and β-carotene content (P values were always >0.152). See Appendix S15 for mean values.

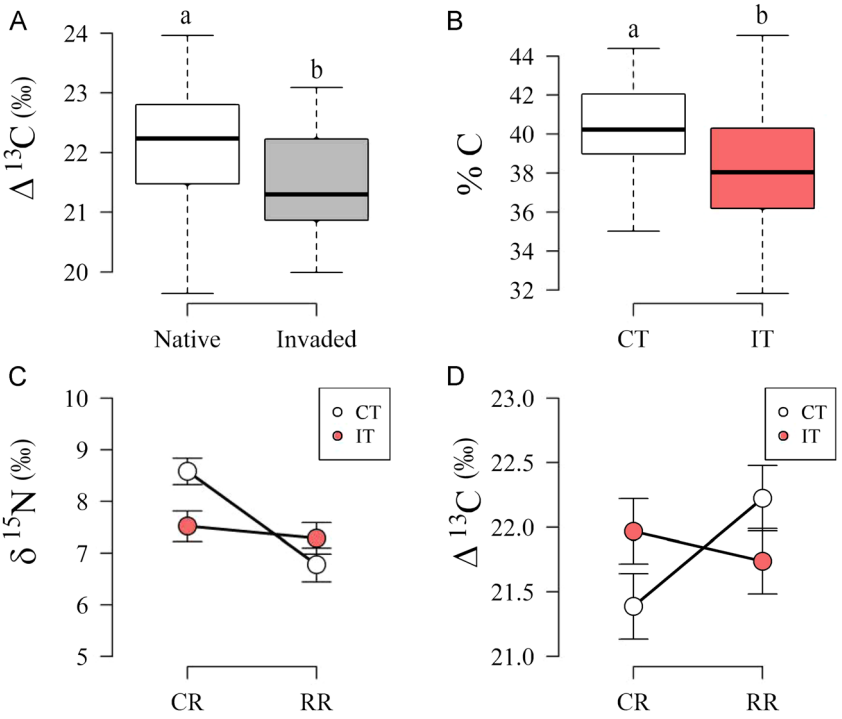

FIGURE 2 (A) Effect of region (native vs. invaded) on carbon isotopic discrimination ($\Delta^{13}C$ [‰]), (B) effect of temperature on C content (C [%]), and (C) combined effects of temperature and rainfall on the nitrogen isotopic composition ($\delta^{15}N$ [‰]) and (D) on the $\Delta^{13}C$ (‰) of *C. edulis* plants. For panels A and B, the boxplots show the median, interquartile range, minimum, maximum, and the suspected outliers; $n = 24$. For panels C and D, values are estimated marginal means (±S.E.; $n = 12$). (CT: control temperature; IT: increased temperature; CR: control rainfall; RR: reduced rainfall). Treatment effects were significant (see text for statistics)

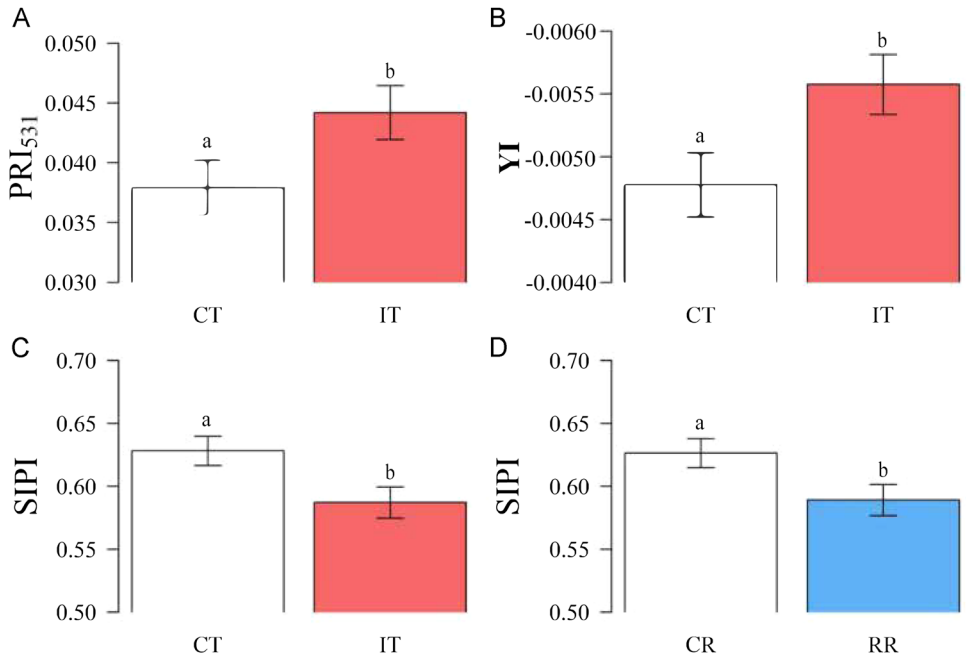

FIGURE 3 Effect of temperature on (A) the photochemical reflectance index (PRI_{531}), the (B) yellowness index (YI), and the (C) structural independent pigment index (SIPI) of *C. edulis* plants and (D) rainfall effect on the SIPI index. (CT: control temperature; IT: increased temperature; CR: control rainfall; RR: reduced rainfall). Values are estimated marginal means of the eight set of measurements (±S.E.; $n = 192$). Different lowercase letters indicate significant differences at $P < 0.05$. See text for statistics, and Appendices S12 and S13 for time-course mean values

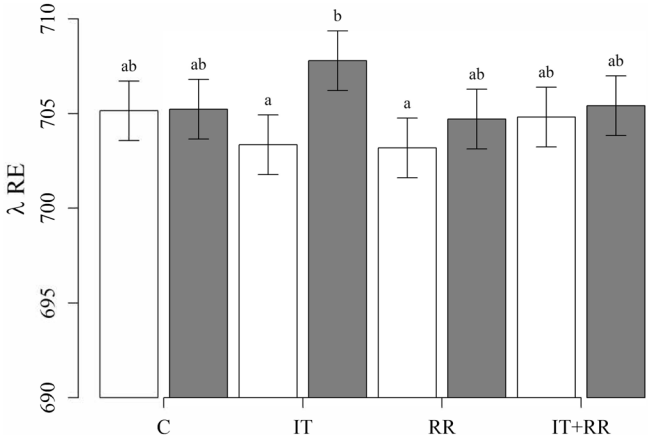

FIGURE 4 Estimated marginal means of the eight set of measurements (±S.E; $n = 48$) showing the effects of temperature (C: control; IT: increased temperature; RR: reduced rainfall; IT + RR: increased temperature and reduced rainfall) on the red edge index (λ RE) of *C. edulis* plants from the native (white bars) and the invaded region (gray bars). Different lowercase letters indicate significant differences at $P < 0.05$ ($F_{1,369} = 5.59$; $P = 0.019$ for the interaction Re × T × R)

Xanthophyll cycle pigments

Although the Zx values were significantly higher in plants from the invaded region than in plants from the native region, the magnitude of the effect depended on temperature and rainfall ($F_{1,39} = 5.87$; $P = 0.020$; $R^2 = 0.33$; Figure 5A). Likewise, the DPS and the VAZ content per chlorophyll unit were both significantly higher in plants from the invaded region than in plants from the native region (VAZ: $F_{1,43} = 6.06$; $P = 0.018$; $R^2 = 0.14$; Figure 5B and DPS: $F_{1,43} = 7.62$; $P = 0.008$; $R^2 = 0.30$; Figure 5C).

Lipid peroxidation, tocopherols, and stress-related phytohormones

The degree of lipid peroxidation was significantly higher in plants from the invaded region than in plants from the native region ($F_{1,42} = 6.23$; $P = 0.017$; $R^2 = 0.20$; see Figure 6A). However, no significant effects of region or climatic treatments on α-TOC and ɤ-TOC were detected (P values were always >0.176).

Irrespective of region, temperature significantly reduced the amount of JA in *C. edulis* ($F_{1,43} = 5.07$; $P = 0.030$; $R^2 = 0.14$; Figure 6B). No significant effects of region or climate conditions on ABA and SA contents were detected (P values were always >0.164). See Appendix S15 for mean values.

DISCUSSION

Responses of *C. edulis* to predicted changes in temperature and rainfall

Our findings show significant effects of temperature and water availability on *C. edulis* growth, physiology, and biochemistry, which could alter the performance of this invasive species under the new climate scenarios. Higher

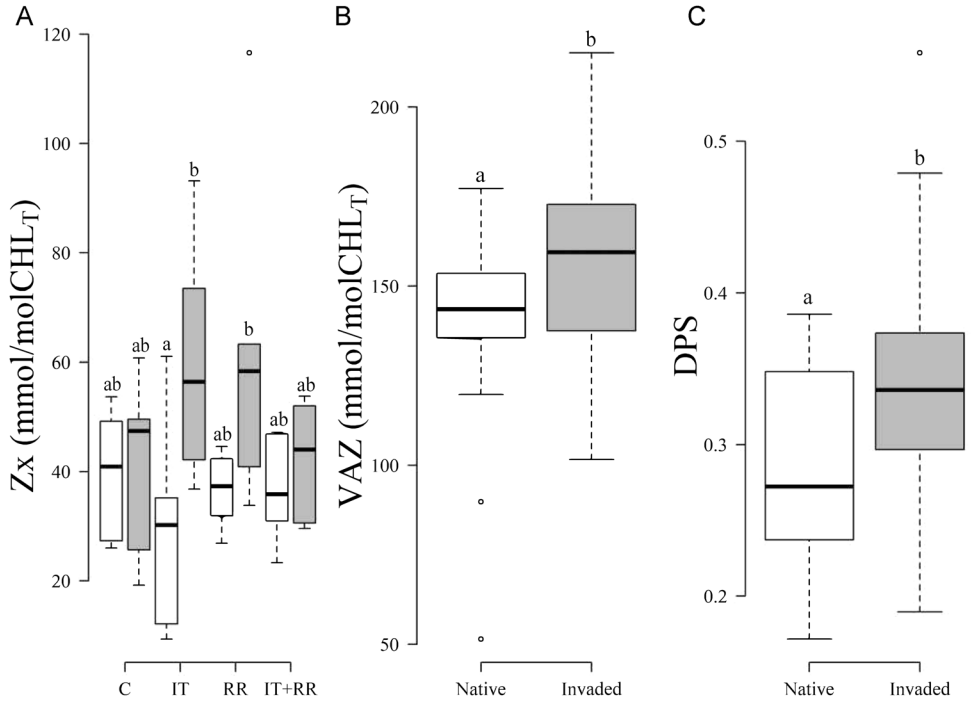

FIGURE 5 (A) Zeaxanthin content (Zx) of *C. edulis* grown in control (C), increased temperature (IT), reduced rainfall (RR), and increased temperature and reduced rainfall (IT+RR) conditions. Panels (B) and (C) show the effect of region (native vs. invaded) on total xanthophyll content (VAZ) and the de-epoxidation state (DPS) of the xanthophyll cycle for *C. edulis*. The boxplots show the median, interquartile range, minimum, maximum, and the suspected outliers; $n = 5$ for (A), and $n = 23$ for (B) and (C). Different lowercase letters indicate significant differences at $P < 0.05$ (see text for statistics)

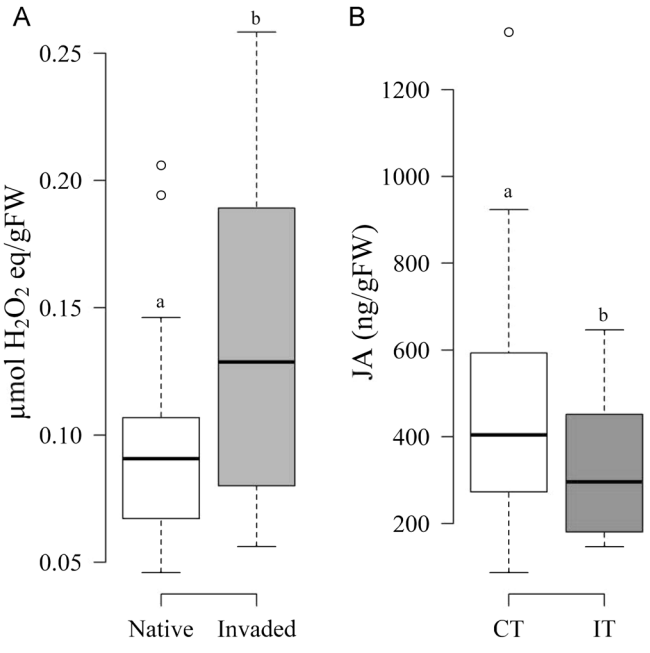

FIGURE 6 (A) Effect of region (native vs. invaded) on the degree of lipid peroxidation of *C. edulis*, and (B) effect of temperature on the jasmonic acid (JA) content of *C. edulis*. The boxplots show the median, interquartile range, minimum, maximum, and the suspected outliers; $n = 22$. Different lowercase letters indicate significant differences at $P < 0.05$ (see text for statistics)

RGR has been widely recognized as a potential determinant of invasion success in plants (Hastings, 1996; Richards et al., 2006). Consistent with our expectations, temperature increased RGR (≈19%) and total dry mass (≈70%), potentially allowing plants to occupy a larger space and therefore have access to a larger portion of limiting resources (Poorter, 1989; Wright et al., 2004). This result strongly suggest that global warming would further promote the invasion of *C. edulis* in Southern Europe by increasing rates of population expansion, intensifying its potential effect on the invaded coastal communities.

Increased temperatures altered the tissue composition in *C. edulis*, significantly decreasing the percentage of C in shoots. According to Lambers et al. (2008) an increase in root temperature would increase the demand for respiratory substrates in roots, resulting in lower carbohydrate concentration in the shoots. Temperature also affected C and N isotopic ratios. In both cases, the effects depended on rainfall, suggesting that the predicted changes in temperature and water availability are likely to affect key processes in C and N cycling (Couto-Vázquez and González-Prieto, 2010). The effect of an increased temperature in intensifying $\Delta^{13}C$ in plants under control rainfall indicates a higher intercellular CO_2 concentration (C_i) at the ribulose-1,5-bisphosphate carboxylase-oxygenase (RuBisCO) active site. Given that the C_i reflects the balance between stomatal conductance (and thus water availability) and

the photosynthetic requirement for carbon dioxide (Farquhar et al., 1989), we interpret that the observed effect is probably due to increased stomatal conductance in these plants to meet the photosynthetic requirement for carbon dioxide. This interpretation is consistent with the observed positive effect of temperature on RGR. We also found that the effect of reduced rainfall in decreasing $\delta^{15}N$ was only manifested in plants under the control temperature, suggesting that the N dynamics in coastal ecosystems could be affected by *C. edulis*. This result contrasts somewhat with observations showing that plant $\delta^{15}N$ signatures increased with increasing aridity (Swap et al., 2004; Wang et al., 2010). However, the large number of factors that cause variations in $\delta^{15}N$ makes comparison across studies difficult, and also hampers precise identification of the N cycle processes that are affected.

Leaf physiological traits can impose limits on plant distribution by determining the range of environments that will potentially be inhabited by a given species (Walter, 1975; Woodward, 1987; Retuerto and Carballeira, 2004). We observed higher photochemical efficiency, lower chlorosis, and lower ratios of carotenoids to chlorophyll *a* in plants under increased temperatures. These results suggest reduced sensitivity of these plants to higher temperatures and consequently lower investment in photoprotection. The PRI is indicative of a photoprotective mechanism that dissipates excess energy via a thermal process that converts violaxanthin to the energy quenching pigments antheraxanthin and zeaxanthin (Gamon et al., 1992). Because this process leads to a reduction in PSII efficiency, PRI_{531} has been correlated with radiation use efficiency (RUE, measured in mol $CO_2 \cdot mol^{-1}$ photons) (Gamon et al., 1992; Peñuelas et al., 1995b). The maximum quantum yield of PSII appears to be more sensitive to the effects of the highest temperatures. In July, when the stress imposed by temperature was most intense, F_v/F_m was significantly lower in plants under increased temperature than in the control plants, with values below 0.75, which is symptomatic of photoinhibition (Bolhàr-Nordenkampf et al., 1989). However, in September, these values recovered fully in *C. edulis* plants under increased temperatures, illustrating the effectiveness of the mechanisms for mitigating heat stress. Fenollosa et al. (2017) described the development of similar photoprotective strategies during the summer in *C. edulis* populations invading the Mediterranean area of the Iberian Peninsula. Our results also revealed higher levels of the JA phytohormone in control plants than in plants under increased temperatures. Several studies have demonstrated a positive role of jasmonate in enhancing constitutive and cold-induced freezing tolerance (see review by Sharma and Laxmi, 2016). *Carpobrotus edulis* is susceptible to freezing injury (MacDonald et al., 1984), and given that jasmonate-induced tolerance to low temperatures may be costly in terms of resources (Van Dam and Baldwin, 1998), the predicted increment in temperature may allow *C. edulis* to forgo these costs, which could instead be invested in growth or reproduction, potentially increasing the invasiveness of this species in the study area. A hypothetical increase in frequency and intensity of cold waves associated with climate change (Francis and Vavrus, 2012) could dampen this effect. However, more recent and compelling research support that global warming will result in a decline in the intensity and frequency of extreme cold spells (Wallace et al., 2014; Freychet et al., 2021).

Regarding water content of the plants, the highest levels of water were maintained during spring and summer. Fenollosa et al. (2017) reported in *C. edulis* a 30% increase in leaf mass per volume (LMV), which is an estimate of leaf succulence, during the summer. Succulence enables plants to survive long periods of water scarcity but also to tolerate high temperatures (Larcher, 1995). The high specific heat of the stored water allows succulent plants such as *C. edulis* to buffer plant tissues against rapid changes in temperature (Fitter and Hay, 2002).

Long-term data of soil salinity recorded in the experimental plot (Hydra Probe SDI 12 sensor; Stevens Water Monitoring Systems Inc., Oregon, USA) showed that the subplots did not differ in salinity so we can be confident that our results were not affected by differences in salinity.

Divergence between native and invasive *C. edulis* populations

A high survival rate of propagules may determine the successful establishment of invasive species (Liu et al., 2014). We found that plants from the invaded region suffered less mortality than the plants from the native region, but contrary to our predictions, we did not detect any significant genotype by environment interaction. This result suggests a higher phenotypic plasticity of the Iberian Peninsula populations supporting greater capacity to adapt to the novel climatic conditions than the South African populations. Subsequently, plants from the invaded region would have evolved in response to the selective pressures experienced in the new environments that led to a divergence from the native plants. We cannot exclude other processes—such as genetic drift, genetic bottlenecks, and admixtures, among others—could contribute to explain the genetic differences observed.

Although previous studies have reported more vigorous growth in invasive populations than in native populations (Blair and Wolfe, 2004; Dlugosch and Parker, 2008), we did not detect any significant differences in the RGR. However, we found that regardless of temperature and rainfall conditions, invading populations diverge from native ones in biomass allocation. It has been suggested that biomechanical and hydrodynamic constraints tend to maintain invariant scaling relationships for intraspecific patterns of biomass allocation (Enquist and Niklas, 2002; Sánchez-Vilas and Retuerto, 2011), but we found that plants from South Africa allocated a higher proportion of biomass to roots than plants from the Iberian Peninsula. Plasticity in allocation can make invasive plants better competitors and it may confer them fitness advantages (Matzek, 2012). Similarly, Portela et al. (2019) demonstrated that biomass partitioning also differed between native and invasive populations of *C. edulis* in response to nutrient availability, suggesting that this trait may be under selection during the process of invasion. Recently,

Smith et al. (2020) concluded that long-distance dispersal and repeated introductions, as occurred with *Carpobrotus* (see review by Campoy et al., 2018), are important to stimulate the formation of new genotypes that may confer adaptive advantages to invasive species in new environments.

The leaf reflectance data suggest that contrary to our predictions, plants from invasive and native populations develop similar physiological responses to the experimental treatments but they differed in their photoprotective strategies. The increased levels of chlorosis (i.e., higher YI values) and lower PRI values observed during the long days of May and June were clearly amplified in plants from native populations. The differential dependence on the thermal quenching pathway shown by native and invasive plants indicates that the greater investment in photoprotection to dissipate the excess light in South African plants may be detrimental to photosynthetic efficiency. This is also consistent with the mean values of the red edge index (ʎ RE), which indicate that the South African plants have a lower chlorophyll content than the Iberian Peninsula plants. Furthermore, native and invasive plants also differed in the state of the xanthophyll cycle in November, as expressed by the PRI values. Colder temperatures in November particularly affected the Iberian Peninsula plants, which showed a greater increase in the VAZ xanthophyll pool than in South African plants. In the same way, as inferred by the higher DPS of invasive plants as a consequence of their higher intrinsic levels of Zx, these plants also showed a higher plastic response, in terms of energy dissipation via the xanthophyll cycle, to the experimental conditions of increased temperature and reduced rainfall in this month. However, biochemical analyses showed similar contents of lutein, β-carotene, and chlorophylls (Chl *a*/*b*, Chl_T) in plants from both regions. Therefore, these results strongly suggest that during the autumn, the Iberian Peninsula plants depended more on the protective action of the xanthophyll cycle than the South African plants, whereas the opposite occurs during the summer. The greater sensitivity of the invasive plants to autumn stress is also supported by their higher lipid peroxidation compared to the native plants, which is indicative of a higher oxidative stress. Fenollosa and Munné-Bosch (2019) compared invasive and native *C. edulis* populations and found an increased sensitivity to chilling in individuals from the native range, with increased de-epoxidation of xanthophylls and accumulation of α-TOC.

Analyses of the intraspecific variability in traits related to the WUE are essential to predict how this species will respond to environmental change. As inferred from our data, WUE was higher in the Iberian Peninsula plants (i.e., a lower $\Delta^{13}C$) than in the South African plants, which is consistent with the lower RSRs ratios observed in the invasive plants. The increased WUE of the Iberian Peninsula plants may guarantee their better performance under the current climate change scenario.

CONCLUSIONS

The effectiveness of physiological mechanisms used by *C. edulis* to cope with the projected climate changes for Southern Europe resulted in higher RGR. Although rainfall modulated the effects of temperature on pigment contents, and N and C isotopic composition, *C. edulis* was less responsive to the influence of reduced rainfall than to the effect of increased temperature. All these changes will probably promote the invasion of *C. edulis* in warmer and drier climates.

Although native and invasive populations did not differ in how they respond to experimentally induced climate change, the significant differences in survival and functional traits between the populations of *C. edulis* from the Iberian Peninsula and South Africa allow us to conclude that the populations have diverged since the species invaded the Iberian Peninsula, more than 100 years ago. Invasive plants would have evolved highly adaptive genotypes in response to the selective pressures experienced in the new environments, leading to divergence from the natives in the pattern of allocation to RSR and in their strategies for photoprotection, and the take up and use of water. The evidence that *C. edulis* may have evolved highly adapted genotypes in just a little over 100 years therefore supports the invasiveness hypothesis whereby new selective pressures may drive rapid genetic changes that favor invasiveness. Finally, our study highlights the fact that analysis of the intraspecific variability in functional traits is essential to aid prediction of how invasive species will respond to climate change.

ACKNOWLEDGMENTS

The authors are grateful to the Spanish Ministry of Economy and Competitiveness and the European Regional Development Fund (ERDF) for funding the study (grants Ref. CGL2013-48885-C2-2-R and Ref. CGL2017-87294-C3-1-P, awarded to R.R.). The authors also thank the authorities of the Parque Nacional Illas Atlánticas (Atlantic Islands National Park), especially J. A. Fernández Bouzas and M. Martínez Morán, for permission to work at the study site, and to the park keepers, Roberto, Pablo, José, and Rosa for logistical support. We are also grateful to the members of the Ecotoxicology and Plant Ecophysiology Group for assistance during the field work, to the Biostatech Company for assistance with data analysis, and to Christine Helen Francis for the English revision. The authors also thank Associate Editor Rebecca Drenovsky and two anonymous reviewers for useful suggestions and comments that greatly improved the manuscript.

AUTHOR CONTRIBUTIONS

R.R., J.G.C., and M.L. designed the study, conducted field sampling, set up the experiment and collected data. R.R. conceived the study and contributed substantially to writing the manuscript. J.G.C. led the analysis, manuscript writing, and submission. S.M. and E.F. performed biochemical analysis and wrote the corresponding parts of the manuscript. All authors commented on and reviewed the final draft.

DATA AVAILABILITY STATEMENT

The final data sets used in this study are available from the FigShare Repository: https://doi.org/10.6084/m9.figshare.14906568.

ORCID

Josefina G. Campoy http://orcid.org/0000-0002-7300-1173
Margarita Lema http://orcid.org/0000-0001-8402-2677
Erola Fenollosa http://orcid.org/0000-0002-6189-2124
Sergi Munné-Bosch http://orcid.org/0000-0001-6523-6848
Rubén Retuerto http://orcid.org/0000-0002-9879-5512

REFERENCES

Adams, M. L., W. D. Philpot, and W. A. Norvell. 1999. Yellowness index: an application of spectral second derivatives to estimate chlorosis of leaves in stressed vegetation. *International Journal of Remote Sensing* 20: 3663–3675.

Allué, A. J. L. 1966. Subregiones fitoclimáticas de España. Ministerio de Agricultura, Dirección General de Montes, Caza y Pesca Fluvial. Instituto Forestal de Investigaciones y Experiencias, Madrid, España.

Amaral, I. F., P. L. Granja, and M. A. Barbosa. 2005. Chemical modification of chitosan by phosphorylation: an XPS, FT-IR and SEM study. *Journal of Biomaterials Science, Polymer Edition* 16: 1575–1593.

Bates, D., M. Mächler, B. Bolker, and S. Walker. 2014. Fitting linear mixed-effects models using lme4. *Journal of Statistical Software* 67: 1–48.

Bellard, C., W. Thuiller, W. Leroy, P. Genovesi, M. Bakkenes, and F. Courchamp. 2013. Will climate change promote future invasions? *Global Change Biology* 19: 3740–3748.

Blair, A. C., and L. M. Wolfe. 2004. The evolution of an invasive plant: an experimental study with *Silene latifolia*. *Ecology* 85: 3035–3042.

Bolhàr-Nordenkampf, H. R., S. P. Long, N. R. Baker, G. Öquist, U. L. E. G. Schreiber, and E. G. Lechner. 1989. Chlorophyll fluorescence as a probe of the photosynthetic competence of leaves in the field: a review of current instrumentation. *Functional Ecology* 3: 497–514.

Bolhàr-Nordenkampf, H. R., and G. Öquist. 1993. Chlorophyll fluorescence as a tool in photosynthesis research. *In* D. O. Hall, J. M. O. Scurlock, H. R. Bolhàr-Nordenkampf, R. C. Leegood, and S. P. Long [eds.], Photosynthesis and production in a changing environment, 193–206. Springer, Dordrecht, Netherlands.

Bourgeois, K., C. M. Suehs, E. Vidal, and F. Médail. 2005. Invasional meltdown potential: facilitation between introduced plants and mammals on French Mediterranean islands. *Ecoscience* 12: 248–256.

Box, G. E. P., and D. R. Cox. 1964. An analysis of transformations. *Journal of the Royal Statistical Society, B, Methodological* 26: 211–252.

Bradley, B. A., D. M. Blumenthal, D. S. Wilcove, and L. H. Ziska. 2010. Predicting plant invasions in an era of global change. *Trends in Ecology & Evolution* 25: 310–318.

Brodersen, C., S. Lavergne, and J. Molofsky. 2008. Genetic variation in photosynthetic characteristics among invasive and native populations of reed canary grass (*Phalaris arundinacea*). *Biological Invasions* 10: 1317–1325.

Campoy, J. G., A. T. R. Acosta, L. Affre, R. Barreiro, G. Brundu, E. Buisson, L. González, et al. 2018. Monographs of invasive plants in Europe: Carpobrotus. *Botany Letters* 165: 440–475.

Campoy, J. G., R. Retuerto, and S. R. Roiloa. 2017. Resource-sharing strategies in ecotypes of the invasive clonal plant *Carpobrotus edulis*: specialization for abundance or scarcity of resources. *Journal of Plant Ecology* 10: 681–691.

Caño, L., J. Escarre, I. Fleck, J. M. Blanco-Moreno, and F. X. Sans. 2008. Increased fitness and plasticity of an invasive species in its introduced range: a study using *Senecio pterophorus*. *Journal of Ecology* 96: 468–476.

Castillo, J. M., B. Gallego-Tévar, E. Figueroa, B. J. Grewell, D. Vallet, H. Rousseau, J. Keller, et al. 2018. Low genetic diversity contrasts with high phenotypic variability in heptaploid *Spartina densiflora* populations invading the Pacific coast of North America. *Ecology and Evolution* 8: 4992–5007.

Castro, M., C. Fernández, and M. A. Gaertner. 1993. Description of a mesoscale atmospheric numerical model. *Mathematics, climate and environment* 27: 230–253.

Chenot, J., L. Affre, A. Passetti, and E. Buisson. 2014. Consequences of iceplant (*Carpobrotus*) invasion on the vegetation and seed bank structure on a Mediterranean island: response elements for their local eradication. *Acta Botanica Gallica* 161: 301–308.

Couto-Vázquez, A., and S. J. González-Prieto. 2010. Effects of climate, tree age, dominance and growth on $\delta^{15}N$ in young pinewoods. *Trees* 24: 507–514.

D'Antonio, C. M. 1990. Seed production and dispersal in the non-native, invasive succulent *Carpobrotus edulis* (Aizoaceae) in coastal strand communities of Central California. *Journal of Applied Ecology* 27: 693–702.

DeLong, J. M., R. K. Prange, D. M. Hodges, C. F. Forney, M. C. Bishop, and M. Quilliam. 2002. Using a modified ferrous oxidation-xylenol orange (FOX) assay for detection of lipid hydroperoxides in plant tissue. *Journal of Agricultural and Food Chemistry* 50: 248–254.

Díez, I., N. Muguerza, A. Santolaria, U. Ganzedo, and J. M. Gorostiaga. 2012. Seaweed assemblage changes in the eastern Cantabrian Sea and their potential relationship to climate change. *Estuarine Coastal and Shelf Science* 99: 108–120.

Dlugosch, K. M., and I. M. Parker. 2008. Invading populations of an ornamental shrub show rapid life history evolution despite genetic bottlenecks. *Ecology Letters* 11: 701–709.

Dukes, J. S., and H. A. Mooney. 1999. Does global change increase the success of biological invaders? *Trends in Ecology & Evolution* 14: 135–139.

EEA. 2017. Climate change, impacts and vulnerability in Europe 2016—an indicator-based report. EEA Report No 1/2017. European Environment Agency, Copenhagen, Denmark.

Ellstrand, N. C., and K. A. Schierenbeck. 2000. Hybridization as a stimulus for the evolution of invasiveness in plants? *Proceedings of the National Academy of Sciences* 97: 7043–7050.

Enquist, B. J., and K. J. Niklas. 2002. Global allocation rules for patterns of biomass partitioning in seed plants. *Science* 295: 1517–1520.

Farquhar, G. D., J. R. Ehleringer, and K. T. Hubick. 1989. Carbon isotope discrimination and photosynthesis. *Annual Review of Plant Physiology and Plant Molecular Biology* 40: 503–537.

Fenollosa, E., A. Gámez, and S. Munné-Bosch. 2019. Plasticity in the hormonal response to cold stress in the invasive plant *Carpobrotus edulis*. *Journal of Plant Physiology* 231: 202–219.

Fenollosa, E., and S. Munné-Bosch. 2019. Increased chilling tolerance of the invasive species *Carpobrotus edulis* may explain its expansion across new territories. *Conservation Physiology* 7: coz075.

Fenollosa, E., S. Munné-Bosch, and M. Pintó-Marijuan. 2017. Contrasting phenotypic plasticity in the photoprotective strategies of the invasive species *Carpobrotus edulis* and the coexisting native species *Crithmum maritimum*. *Physiologia Plantarum* 160: 185–200.

Filella, I., and J. Peñuelas. 1994. The red edge position and shape as indicators of plant chlorophyll content, biomass and hydric status. *International Journal of Remote Sensing* 15: 1459–1470.

Fitter, A. H., and R. K. M. Hay. 2002. Environmental physiology of plants. Academic Press, San Diego, California, USA.

Francis, J. A., and S. J. Vavrus. 2012. Evidence linking Arctic amplification to extreme weather in mid-latitudes. *Geophysical Research Letters* 39: L06801.

Freychet, N., S. F. B. Tett, A. A. Abatan, A. Schurer, and Z. Feng. 2021. Widespread persistent extreme cold events over South-East China: Mechanisms, trends and attribution. *Journal of Geophysical Research: Atmospheres* 126: e2020JD033447.

Gamon, J. A., J. Peñuelas, and C. B. Field. 1992. A narrow-waveband spectral index that tracks diurnal changes in photosynthetic efficiency. *Remote Sensing of Environment* 41: 35–44.

Gomez, D. 2006. AVICOL, A program to analyse spectrometric data. Website: http://sites.google.com/site/avicolprogram. Free executable also available from the author at dodogomez@yahoo.fr

Gonçalves, M. L. 1990. *Carpobrotus* N.E. Br. *In* S. Castroviejo, M. Laínz, G. López González, P. Montserrat, F. Muñoz Garmendia, J. Paiva, and L. Villar [eds.], Flora Iberica. Plantas vascualres de la Península Ibérica e Islas Baleares, Vol. II, 82–85. C.S.I.C, Madrid, Spain.

Guo, J. M., and C. M. Trotter. 2004. Estimating photosynthetic light-use efficiency using the photochemical reflectance index: variations among species. *Functional Plant Biology* 31: 255–265.

Harper, J. L. 1977. Population biology of plants. Academic Press, London, United Kingdom.

Hastings, A. 1996. Models of spatial spread: a synthesis. *Biological Conservation* 78: 143–148.

Hollister, R. D., and P. J. Webber. 2000. Biotic validation of small open-top chambers in a tundra ecosystem. *Global Change Biology* 6: 835–842.

Hulme, P. E. 2008. Phenotypic plasticity and plant invasions: is it all Jack? *Functional Ecology* 22: 3–7.

IGME. 2014. Guía geológica del Parque Nacional de las Islas Atlánticas de Galicia (Guías Geológicas de Parques Nacionales). Organismo Autónomo de Parques Nacionales [ed]. Instituto Geológico y Minero de España, Editorial Everest S.A, Spain, 202 pp.

IPCC. 2014. Climate Change 2014: Synthesis Report. Contribution of Working Groups I, II and III to the Fifth Report of the Intergovernmental Panel on Climate Change (Core Writing Team, R. K. Pachauri, and L. A. Meyer [eds.]). IPCC, Geneva, Switzerland, 151 pp.

Kottek, M., J. Grieser, C. Beck, B. Rudolf, and F. Rubel. 2006. World map of the Köppen-Geiger climate classification updated. *Meteorologische Zeitschrift* 15: 259–263.

Lambers, H., F. S. I. Chapin, and T. L. Pons. 2008. Plant physiological ecology. Springer, New York, New York, USA.

Larcher, W. 1995. Physiological plant ecology. Springer-Verlag, Berlin, Heidelberg, Germany.

Lee, C. E. 2002. Evolutionary genetics of invasive species. *Trends in Ecology & Evolution* 17: 386–391.

Lenth, R. 2019. emmeans: estimated marginal means, aka least-squares means. Website: https://cran.r-project.org/package=emmeans

Lichtenthaler, H. K., A. Gitelson, and M. Lang. 1996. Non-destructive determination of chlorophyll content of leaves of a green and an aurea mutant of tobacco by reflectance measurements. *Journal of Plant Physiology* 148: 483–493.

Liu, R. H., Q. W. Chen, B. C. Dong, and F. H. Yu. 2014. Effects of vegetative propagule pressure on the establishment of an introduced clonal plant, *Hydrocotyle vulgaris*. *Scientific Reports* 4: 1–6.

MacDonald, J. D., J. R. Hartman, and J. D. Shapiro. 1984. Pathogens of ice plant in California. *Plant Disease* 68: 965–967.

Mack, R. N., D. Simberloff, M. W. Lonsdale, H. Evans, M. Clout, and F. A. Bazzaz. 2000. Biotic invasions: causes, epidemiology, global consequences, and control. *Ecological applications* 10: 689–710.

Maestre, F. T., C. Escolar, M. L. Guevara, J. L. Quero, R. Lázaro, M. Delgado-Baquerizo, V Ochoa, et al. 2013. Changes in biocrust cover drive carbon cycle responses to climate change in drylands. *Global Change Biology* 19: 3835–3847.

Maron, J. L., S. C. Elmendorf, and M. Vilà. 2007. Contrasting plant physiological adaptation to climate in the native and introduced range of *Hypericum perforatum*. *Evolution* 61: 1912–1924.

Matesanz, S., E. Gianoli, and F. Valladares. 2010. Global change and the evolution of phenotypic plasticity in plants. *In* C. D. Schlichting, and T. A. Mousseau [eds.], Annals of the New York Academy of Sciences, Year in Evolutionary Biology, Vol. 1206, 35–55. New York Academy of Sciences, New York, New York, USA.

Matesanz, S., and F. Valladares. 2014. Ecological and evolutionary responses of Mediterranean plants to global change. *Environmental and Experimental Botany* 103: 53–67.

Matzek, V. 2012. Trait values, not trait plasticity, best explain invasive species' performance in a changing environment. *PLoS One* 7: e48821.

Mostert, E., M. Gaertner, P. M. Holmes, A. G. Rebelo, and D. M. Richardson. 2017. Impacts of invasive alien trees on threatened lowland vegetation types in the Cape Floristic Region, South Africa. *South African Journal of Botany* 108: 209–222.

Müller, M., and S. Munné-Bosch. 2011. Rapid and sensitive hormonal profiling of complex plant samples by liquid chromatography coupled to electrospray ionization tandem mass spectrometry. *Plant Methods* 7: 37.

Munné-Bosch, S., and L. Alegre. 2000. Changes in carotenoids, tocopherols and diterpenes during drought and recovery, and the biological significance of chlorophyll loss in *Rosmarinus officinalis* plants. *Planta* 210: 925–931.

Nguyen, M. A., A. E. Ortega, K. Q. Nguyen, S. Kimball, M. L. Goulden, and J. L. Funk. 2016. Evolutionary responses of invasive grass species to variation in precipitation and soil nitrogen. *Journal of Ecology* 104: 979–986.

Peñuelas, J., F. Baret, and I. Filella. 1995a. Semi-empirical indices to assess carotenoids chlorophyll-*a* ratio from leaf spectral reflectance. *Photosynthetica* 31: 221–230.

Peñuelas, J., I. Filella, and J. A. Gamon. 1995b. Assessment of photosynthetic radiation-use efficiency with spectral reflectance. *The New Phytologist* 131: 291–296.

Peñuelas, J., and I. Filella. 1998. Visible and near-infrared reflectance techniques for diagnosing plant physiological status. *Trends in Plant Science* 3: 151–156.

Peñuelas, J., J. Pinol, R. Ogaya, and I. Filella, 1997. Estimation of plant water concentration by the reflectance water index WI (R900/R970). *International Journal of Remote Sensing* 18: 2869–2875.

Poorter, H. 1989. Interspecific variation in relative growth rate: on ecological causes and physiological consequences. *In* H. Lambers, M. L. Cambridge, H. Konings, and T. L. Pons [eds.], Causes and consequences of variation in growth rate and productivity of higher plants, Vol. 24, 45–68. SPB Academic Publishing BV, The Hague, Netherlands.

Portela, R., R. Barreiro, and S. R. Roiloa. 2019. Biomass partitioning in response to resources availability: a comparison between native and invaded ranges in the clonal invader *Carpobrotus edulis*. *Plant Species Biology* 34: 11–18.

R Core Team. 2015. R: A language and environment for statistical computing. R Foundation for Statistical Computing, Vienna, Austria.

Retuerto, R., and A. Carballeira. 2004. Estimating plant responses to climate by direct gradient analysis and geographic distribution analysis. *Plant Ecology* 170: 185–202.

Richards, C. L., O. Bossdorf, N. Z. Muth, J. Gurevitch, and M. Pigliucci. 2006. Jack of all trades, master of some? On the role of phenotypic plasticity in plant invasions. *Ecology Letters* 9: 981–993.

Roiloa, S. R., R. Retuerto, J. G. Campoy, A. Novoa, and R. Barreiro. 2016. Division of labor brings greater benefits to clones of *Carpobrotus edulis* in the non-native range: evidence for rapid adaptive evolution. *Frontiers in Plant Science* 7: 349.

Sala, O. E., F. S. Chapin, J. J. Armesto, E. Berlow, J. Bloomfield, R. Dirzo, E. Huber-Sanwald et al. 2000. Global biodiversity scenarios for the year 2100. *Science* 287: 1770–1774.

Sánchez-Vilas, J., and R. Retuerto. 2011. Reproduction reduces photosynthetic capacity in females of the subdioecious *Honckenya peploides*. *Acta Oecologica* 37: 155–163.

Sax, D. F., J. J. Stachowicz, J. H. Brown, J. F. Bruno, M. N. Dawson, S. D. Gaines, R. K. Grosberg, et al. 2007. Ecological and evolutionary insights from species invasions. *Trends in Ecology & Evolution* 22: 465–471.

Schröter, D., W. Cramer, R. Leemans, I. C. Prentice, M. B. Araújo, N. W. Arnell, A. Bondeau et al. 2005. Ecosystem service supply and vulnerability to global change in Europe. *Science* 310: 1333–1337.

Sharma, M., and A. Laxmi. 2016. Jasmonates: emerging players in controlling temperature stress tolerance. *Frontiers in Plant Science* 6: 1129.

Smith, A. L., T. R. Hodkinson, J. Villellas, J. A. Catford, A. M. Csergő, S. P. Blomberg, E. E. Crone, et al. 2020. Global gene flow releases invasive plants from environmental constraints on genetic diversity. *Proceedings of the National Academy of Sciences* 117: 4218–4227.

Suehs, C. M., L. Affre, and F. Médail. 2004. Invasion dynamics of two alien *Carpobrotus* (Aizoaceae) taxa on a Mediterranean Island: II. Reproductive strategies. *Heredity* 92: 550–556.

Swap, R. J., J. N. Aranibar, P. R. Dowty, W. P. Gilhooly, and S. A. Macko. 2004. Natural abundance of ^{13}C and ^{15}N in C_3 and C_4 vegetation of southern Africa: patterns and implications. *Global Change Biology* 10: 350–358.

Therneau, T. M. 2021. A package for survival analysis in R. Website: https://cran.r-project.org/package=survival

Therneau, T. M., and P. M. Grambsch. 2000. The Cox model. *In* Modeling survival data: extending the Cox model, 39–77. Springer-Verlag, New York, New York, USA.

Thompson, J. N. 1998. Rapid evolution as an ecological process. *Trends in Ecology & Evolution* 13: 329–332.

Thuiller, W., D. M. Richardson, and G. F. Midgley. 2007. Will climate change promote alien plant invasions? *In* W. Nentwig [ed.], Biological Invasions, Vol. 193, 197–211. Springer-Verlag, Berlin, Heidelberg, Germany.

Thuiller, W., D. M. Richardson, P. Pyšek, G. F. Midgley, G. O. Hughes, and M. Rouget. 2005. Niche-based modelling as a tool for predicting the risk of alien plant invasions at a global scale. *Global Change Biology* 11: 2234–2250.

Van Dam, N. M., and I. T. Baldwin. 1998. Costs of jasmonate-induced responses in plants competing for limited resources. *Ecology Letters* 1: 30–33.

Vilà, M., and C. M. D'Antonio. 1998. Hybrid vigor for clonal growth in *Carpobrotus* (Aizoaceae) in coastal California. *Ecological Applications* 8: 1196–1205.

Villar, R., J. Ruiz-Robleto, J. L. Quero, H. Poorter, F. Valladares, and T. Marañón. 2004. Tasas de crecimiento en especies leñosas: aspectos funcionales e implicaciones ecológicas. *In* F. Valladares [ed.], Ecología del bosque mediterráneo en un mundo cambiante, 191–227. Ministerio de Medio Ambiente, EGRAF, S. A., Madrid, Spain.

Vitousek, P. M., C. M. D'Antonio, L. L. Loope, M. Rejmanek, and R. Westbrooks. 1997. Introduced species: a significant component of human-caused global change. *New Zealand Journal of Ecology* 21: 1–16.

Wallace, J. M., I. M. Held, D. W. Thompson, K. E. Trenberth, and J. E. Walsh. 2014. Global warming and winter weather. *Science* 343: 729–730.

Walter, J. H. 1975. Vegetation of the earth in relation to climate and the eco-physiological conditions. *Folia Geobotanica et Phytotaxonomica* 10: 100.

Walther, G. R., A. Roques, P. E. Hulme, M. T. Sykes, P. Pyšek, I. Kühn, M. Zobel, et al. 2009. Alien species in a warmer world: risks and opportunities. *Trends in Ecology & Evolution* 24: 686–693.

Wang, L. X., P. D'Odorico, L. Ries, and S. A. Macko. 2010. Patterns and implications of plant-soil $\delta^{13}C$ and $\delta^{15}N$ values in African savanna ecosystems. *Quaternary Research* 73: 77–83.

Winter, K., and J. A. M. Holtum. 2014. Facultative crassulacean acid metabolism (CAM) plants: powerful tools for unravelling the functional elements of CAM photosynthesis. *Journal of Experimental Botany* 65: 3425–3441.

Wisura, W., and H. F. Glen. 1993. The South African species of *Carpobrotus* (Mesembryanthema–Aizoaceae). *Contributions to the Bolus Herbarium* 15: 76–107.

Woodward, F. I. 1987. Climate and plant distribution (Cambridge studies in Ecology). Cambridge University Press, Cambridge, UK.

Wright, I. J., P. B. Reich, M. Westoby, D. D. Ackerly, Z. Baruch, F. Bongers, J. Cavender-Bares, et al. 2004. The worldwide leaf economics spectrum. *Nature* 428: 821–827.

Yahdjian, L., and O. E. Sala. 2002. A rainout shelter design for intercepting different amounts of rainfall. *Oecologia* 133: 95–101.

SUPPORTING INFORMATION

Additional supporting information may be found in the online version of the article at the publisher's website.

Appendix S1. Detailed view of *C. edulis* growing on the island of Sálvora (northwest of the Iberian Peninsula).

Appendix S2. Location of the study area in the northeast of the island of Sálvora and general view of the experimental plot within the Atlantic Islands National Park (Galicia) (northwest of the Iberian Peninsula).

Appendix S3. Detailed views of the experimental plot with regularly demarcated 32 subplots inside, separated from each other by approximately 1.2 m.

Appendix S4. View of experimental subplots showing an example of an open top chamber (OTC) for (a) increased temperature, (b) reduced rainfall subplot, (c) OTC and reduced rainfall subplot, and (d) control unmodified climate subplot. The water intercepted by the rainfall collectors was channeled through (e) a flexible pipe into (f) storage tanks.

Appendix S5. Site location of *Carpobrotus edulis* populations sampled from the invaded region in South Europe (1: Viveiro, Spain; 2: Caminha, Portugal; 3: Castelo do Neiva, Portugal; 4: Quiaios, Portugal) and from the native region in South Africa (5: Cape of Good Hope; 6: Fish Hoek; 7: Kleinmond; 8: Hawston).

Appendix S6. Panels (a) and (b) show the effects of predation by small rodents and the scale insect *Pulvinariella mesembryanthemi* (Vallot, 1828) on ramets of *C. edulis* growing inside the plot, and panels (c) and (d) are detailed views of the different sensors used to monitor the atmospheric conditions (air and soil temperature and relative humidity) in the experimental subplots.

Appendix S7. Effects of the experimental treatments (differences in increased temperature, [IT], reduced rainfall [RR], and increased temperature and reduced rainfall [IT+RR], relative to the control treatment) on (a) air temperature and (b) relative air humidity. Air temperature and relative humidity in the control treatment throughout the duration of the experiment are shown in panels (c) and (d). Values are means of daily air temperature and humidity.

Appendix S8. Effects of the experimental treatments (differences in increased temperature, [IT], reduced rainfall [RR]), and increased temperature and reduced rainfall [IT+RR], relative to the control treatment) on (a) soil temperature and (b) soil humidity. Soil temperature and humidity in the control treatment throughout the duration of the experiment are shown in panels (c) and (d). Values are means of daily soil temperature and humidity.

Appendix S9. Daily air temperature (°C) and rainfall (L/m^2) between 2015–2016 recorded at the Sálvora meteorological station. Data provided by MeteoGalicia, Consellería de Medio Ambiente, Territorio e Infraestruturas (Xunta de Galicia).

Appendix S10. Effect of region of ramet collection on the survival probability of *C. edulis* plants between the beginning (September 2015) and the end of the experiment (November 2016). Lines represent the semiparametric Cox proportional hazards models and dots represent the Kaplan-Meier estimator for the survival functions of plants from the invaded (green) and native (red) regions.

Appendix S11. Boxplots showing the distribution of data (median, interquartile range, minimum, maximum, and the suspected outliers; $n = 6$) for growth measurements: (a) relative growth rate (RGR [year^{-1}]), (b) total dry mass [g], (c) root dry mass [g], and (d) root-to-shoot ratio [RSR]), of *C. edulis* from native (white bars) and invaded (gray bars) regions, grown under control (C), increased temperature (IT), reduced rainfall (RR), and increased temperature with reduced rainfall (IT+RR) conditions.

Appendix S12. Boxplots showing the distribution of data (median, interquartile range, minimum, maximum, and the suspected outliers; $n = 6$) for the composition of plant tissues: (a) C/N, (b) $\Delta^{13}C$ (‰), and (c) $\delta^{15}N$ (‰), of *C. edulis* from native (white bars) and invaded (gray bars) regions, under control (C), increased temperature (IT), reduced rainfall (RR), and increased temperature with reduced rainfall (IT+RR) conditions.

Appendix S13. Time-course values of physiological parameters: (a) photochemical reflectance index (PRI_{531}), (b) red edge index (λ RE), (c) yellowness index (YI), (d) structural independent pigment index (SIPI), and (e) maximum quantum yield (F_v/F_m), for *C. edulis* between November 2015 and November 2016. White and red (black) dots show plants grown under control temperature (CT), and increased temperature (IT) conditions. Values are means (±S.E.; $n = 24$).

Appendix S14. Boxplots showing the distribution of data (median, interquartile range, minimum, maximum, and the suspected outliers; $n = 6$) of seasonal measurements throughout the experiment (between November 2015 and November 2016) for the (a) photochemical reflectance index (PRI_{531}), (b) red edge index (λ RE), (c) yellowness index (YI), (d) structural independent pigment index (SIPI), (e) water index (WI_{900}), and (f) maximum quantum yield (F_v/F_m) of *C. edulis* from native (white bars) and invaded (gray bars) regions, under control (C), increased temperature (IT), reduced rainfall (RR), and increased temperature with reduced rainfall (IT+RR) conditions.

Appendix S15. Mean values (±S.E; $n = 6$) of the chlorophyll contents (Chl_T, Chl *a*/*b*, carotenoids [Car]/Chl_T in nmol/cm^2), xanthophyll pigments (violaxanthin [Vx], antheraxanthin [Ax], and zeaxanthin [Zx], total xanthophyll contents [VAZ], de-epoxidation state of the xanthophyll cycle [DPS], lutein [Lut], and β-carotene [β-car], in mmol/mol Chl_T), stress-related phytohormones (abscisic acid [ABA], jasmonic acid [JA], and salicylic acid [SA] in parts per billion [ppb]: ng/gFW), tocopherols content (α-TOC and ϒ-TOC in nmol/gFW), and the degree of lipid peroxidation (in μmol H_2O_2eq/gFW), for *C. edulis* plants from the native and invaded regions as a function of temperature (T) and rainfall (R). CT and IT mean control and increased temperature, respectively, and CR and RR control and reduced rainfall conditions, respectively.

How to cite this article: Campoy, J. G., M. Lema, E. Fenollosa, S. Munné-Bosch, and R. Retuerto. 2021. Functional responses to climate change may increase invasive potential of *Carpobrotus edulis*. *American Journal of Botany* 108(10): 1902–1916. https://doi.org/10.1002/ajb2.1745